



HAL
open science

Adipocyte Reprogramming by the Transcriptional Coregulator GPS2 Impacts Beta Cell Insulin Secretion

Karima Drareni, Raphaëlle Ballaire, Fawaz Alzaid, Andreia Goncalves, Catherine Chollet, Serena Barilla, Jean-Louis Nguewa, Karine Dias, Sophie Lemoine, Jean-Pierre Riveline, et al.

► **To cite this version:**

Karima Drareni, Raphaëlle Ballaire, Fawaz Alzaid, Andreia Goncalves, Catherine Chollet, et al.. Adipocyte Reprogramming by the Transcriptional Coregulator GPS2 Impacts Beta Cell Insulin Secretion. Cell Reports, 2020, 32, pp.108141 -. 10.1016/j.celrep.2020.108141 . hal-03491495

HAL Id: hal-03491495

<https://hal.science/hal-03491495>

Submitted on 21 Sep 2022

HAL is a multi-disciplinary open access archive for the deposit and dissemination of scientific research documents, whether they are published or not. The documents may come from teaching and research institutions in France or abroad, or from public or private research centers.

L'archive ouverte pluridisciplinaire **HAL**, est destinée au dépôt et à la diffusion de documents scientifiques de niveau recherche, publiés ou non, émanant des établissements d'enseignement et de recherche français ou étrangers, des laboratoires publics ou privés.



Distributed under a Creative Commons Attribution - NonCommercial 4.0 International License

2 **Adipocyte Reprogramming by the Transcriptional Coregulator GPS2 Impacts Beta Cell** 3 **Insulin Secretion**

4
5 Karima Drareni¹, Raphaëlle Ballaire², Fawaz Alzaid¹, Andreia Goncalves¹, Catherine Chol-
6 let¹, Serena Barilla⁶, Jean-Louis Nguewa³, Karine Dias⁴, Sophie Lemoine⁴, Riveline Jean-
7 Pierre^{1,3}, Ronan Roussel^{1,5}, Elise Dalmas¹, Gilberto Velho¹, Eckardt Treuter⁶, Jean-François
8 Gautier^{1,3} and Nicolas Venteclef^{1,7}.

9
10 ¹Cordeliers Research Centre, INSERM, Immunity and Metabolism in Diabetes Laboratory,
11 Université de Paris, F-75006, Paris, France.

12 ²Inovarian, Paris, France

13 ³Department of Diabetes, Clinical Investigation Centre (CIC-9504), Lariboisière Hospital,
14 Assistance Publique - Hôpitaux de Paris, Paris, France.

15 ⁴École normale supérieure, PSL Research University, Centre National de la Recherche Scien-
16 tifique (CNRS), INSERM, Institut de Biologie de l'École Normale Supérieure (IBENS), Pla-
17 teforme Génomique, Paris, France.

18 ⁵Department of Diabetology, Endocrinology and Nutrition, DHU FIRE, Bichat Hospital, As-
19 sistance Publique - Hôpitaux de Paris, Paris, France

20 ⁶Department of Biosciences and Nutrition, Karolinska Institutet, Huddinge, 14157, Sweden

21 ⁷Lead contact

22
23 Correspondence:

24 Karima Drareni:

25 Cordeliers Research Centre, INSERM, Immunity and Metabolism in Diabetes Laboratory,
26 Université de Paris, F-75006, Paris, France.

27 karimadrareni@gmail.com

28 Nicolas Venteclef :

29 Cordeliers Research Centre, INSERM, Immunity and Metabolism in Diabetes Laboratory,
30 Université de Paris, F-75006, Paris, France.

31 nicolas.venteclef@inserm.fr

32 **ABSTRACT**

33 Glucose homeostasis is maintained through organ crosstalk that regulates secretion of insulin
34 to keep blood glucose levels within a physiological range. In type 2 diabetes, this coordinated
35 response is altered, leading to a deregulation of beta cell function and inadequate insulin se-
36 cretion. Reprogramming of white adipose tissue has a central role in this deregulation, but the
37 critical regulatory components remain unclear. Here, we demonstrate that expression of the
38 transcriptional coregulator GPS2 in white adipose tissue is correlated with insulin secretion
39 rate in humans. The causality of this relationship is confirmed using adipocyte-specific GPS2
40 knockout mice, in which inappropriate secretion of insulin promotes glucose intolerance. This
41 phenotype is driven by adipose tissue-secreted factors, which cause increased pancreatic islet
42 inflammation and impaired beta cell function. Thus, our study suggests that in mice and in
43 humans, GPS2 controls the reprogramming of white adipocytes to influence pancreatic islet
44 function and insulin secretion.

45

46

47 **Keywords:** Type 2 diabetes, adipose tissue, organ crosstalk, pancreas, beta cells, insulin,
48 transcriptional coregulator, G protein pathway suppressor 2, GPS2

49

50

51

52

53 INTRODUCTION

54 Metabolic homeostasis is regulated by the coordinated action of multiple organ systems. The
55 central principle of glucose homeostasis is that pancreatic beta cells secrete insulin in re-
56 sponse to glucose, and insulin acts upon target tissues such as the liver, muscle and adipose
57 tissue to reduce blood glucose levels. However, in addition to glucose, beta cells respond to a
58 vast array of metabolic and endocrine signals including lipids, hormones and cytokines
59 (Scharfmann et al., 2019). Therefore, beta cells integrate a plethora of systemic signals that
60 reflect the metabolic status and secrete appropriate amounts of insulin to maintain metabolic
61 homeostasis. In type 2 diabetes, this metabolic homeostasis is disturbed leading to the mala-
62 daptation of beta cells characterized by inappropriate secretion of insulin and glucose intoler-
63 ance. In this pathophysiological context, white adipose tissue (WAT) is an essential endocrine
64 organ that contributes to maintain glucose homeostasis by secreting factors such as adiponec-
65 tin that optimizes insulin secretion and action (Romacho et al., 2014). However, in obesity,
66 WAT plays a key function in disturbing glucose homeostasis by secreting factors that affect
67 the function of cells and tissues throughout the body including beta cells (Kita et al., 2019;
68 Marcelin et al., 2019). During the development of obesity, WAT undergoes morphological
69 and cellular changes leading to adipocyte hypertrophy, WAT inflammation and hypoxia,
70 which represent hallmarks of maladaptive WAT expansion in obesity. This maladaptive WAT
71 expansion has been associated with numerous deleterious cardio-metabolic complications
72 including type 2 diabetes in humans (Muir et al., 2016; Romacho et al., 2014). Others and we
73 recently proposed that the transcriptional coregulator GPS2, subunit of the chromatin-
74 modifying HDAC3 corepressor complex (Treuter et al., 2017) influences adipocyte functions
75 in the context of obesity and type 2 diabetes (Cardamone et al., 2012; Cardamone et al., 2018;
76 Cardamone et al., 2014; Cederquist et al., 2017; Drareni et al., 2018; Fan et al., 2016; Toubal
77 et al., 2013). By studying human WAT, we previously reported that reduced expression of
78 GPS2 in adipocytes coincides with the increased expression of inflammatory (IL6 and MCP1)
79 and hypoxic (HIF1A) genes, and hypertrophic adipocytes (Drareni et al., 2018; Toubal et al.,
80 2013). Our functional analysis further revealed that adipocyte-specific loss of GPS2 triggers
81 transcriptional alterations of inflammatory and remodeling gene signatures in WAT, leading
82 to a pro-diabetic status characterized by insulin resistance and glucose intolerance.

83 Here, we discover a previously unrecognized adipocyte-specific role of GPS2 in the regula-
84 tion of insulin secretion from beta cells. We report that GPS2 mRNA levels in WAT correlate
85 with the insulin secretion rate in humans. Mechanistic studies revealed that the loss of GPS2
86 in adipocyte-specific knockout (AKO) mice provokes an inadequate adaption of pancreatic

87 beta cells, leading to decreased insulin secretion in obese mice. *Ex vivo* assays revealed that
88 the WAT secretome of obese GPS2 AKO mice interferes with beta cell function, leading to a
89 reduction of insulin secretion upon glucose stimulation. Collectively, our study reveals that
90 the loss of GPS2 in adipocytes impacts beta cell adaptation and insulin secretion during the
91 progression of obesity and type 2 diabetes.

92

93 **RESULTS**

94

95 **Potential Impact of GPS2 Function in WAT in Insulin Secretion Rate in Humans**

96 To evaluate the impact of GPS2 action in WAT onto insulin secretion rates (ISR) in humans,
97 we measured the mRNA levels of GPS2 in subcutaneous WAT (scWAT) of 23 clinical study
98 participants (8 with normal glucose tolerance and 15 with type 2 diabetes; aged 48 ± 12 years;
99 men 68%), which were subjected to graded glucose infusion in order to measure ISR (**Table**
100 **S1**). Each subject received a stepped intravenous (IV) glucose infusion at 2, 4, 6, 8 and 10
101 mg/kg/min, each step lasting for 40 min. ISR was derived by deconvolution of peripheral C-
102 peptide levels. Participants were stratified according to GPS2 mRNA expression in scWAT,
103 quantified by RT-qPCR, into two categories, low (L_{exp}) or high expression (H_{exp}), defined by
104 values below or above the median, respectively (**Table S1**). Basal glucose levels and ISR
105 were higher in L_{exp} than in H_{exp} participants: 8.0 ± 0.5 vs 5.6 ± 0.3 mmol/l, mean \pm SEM,
106 $p=0.0008$, and 3.04 ± 0.19 vs 2.12 ± 0.17 pmol/kg/min, $p=0.002$, respectively (**Figure S1**). Fol-
107 lowing glucose infusion, glucose levels increased $178 \pm 17\%$ and $174 \pm 23\%$ ($p=0.88$) in L_{exp}
108 and H_{exp} participants, with average values of 14.9 ± 0.6 and 11.4 ± 0.78 mmol/l ($p=0.002$), re-
109 spectively. Concomitant ISR levels increased $236 \pm 40\%$ and $487 \pm 75\%$ ($p=0.006$) in L_{exp} and
110 H_{exp} participants. Average ISR following glucose infusion was 5.40 ± 0.67 vs 8.49 ± 0.75
111 pmol/kg/min, $p=0.01$, respectively (**Figure S1**). Analysis of the glucose/ISR response curve
112 demonstrated significantly higher ISR in H_{exp} than in L_{exp} participants at all glucose levels
113 ($p=0.005$, adjusted for sex, age, BMI, and glycemic status) (**Figure 1A**). It was $\sim 52\%$, $\sim 60\%$
114 and $\sim 45\%$ higher at 7, 10 and 15 mmol/l glucose, respectively. Average ISR (time 10 to 200
115 min) was well correlated with GPS2 mRNA expression in scWAT (**Figure 1B**).

116 Acute insulin, glucagon and C-peptide were also quantified during glucose-dependent argi-
117 nine stimulation. We observed that the acute secretion of insulin and C-peptide in partici-
118 pants with high GPS2 expression in WAT was more pronounced than in participants with low
119 expression. In mirror, Glucagon secretion was less pronounced in the high expression group
120 than in the low expression group (**Figure S1**). Importantly, multivariate correlative analyses

121 between GPS2 expressions in WAT with acute insulin secretion demonstrated a significant
122 positive correlation between WAT GPS2 mRNA levels and acute insulin secretion ($R^2=0,31$,
123 $p=0,03$, adjusted for sex, age, glycaemic status, pre-arginine glucose levels) (**Figure 1C**).
124 However, we did not observe correlation between WAT GPS2 mRNA levels and acute gluca-
125 gon secretion ($R^2=0.04$, $p=0.88$, adjusted for sex, age, glycaemic status, pre-arginine glucose
126 levels) (**Figure S1**). Collectively, these results suggest a potential impact of GPS2 function in
127 WAT on the insulin secretion response to glucose but not to the secretion of glucagon.
128 Similar associations were observed in mice. Stratification of 18 high-fat fed mice according to
129 *Gps2* expression in WAT revealed that *Gps2* low expressers are more glucose intolerant than
130 *Gps2* high expressers (**Figures 2A and 2B, Figures S2A and S2B**). The glucose intolerance
131 observed in *Gps2* low expressers correlated with a decreased glucose-stimulated insulin secre-
132 tion (**Figure 2C and 2D**), while the insulin resistance status (based on HOMA-IR) was simi-
133 lar between the groups (**Figure S2C**). Importantly, we could not observe these correlations by
134 stratifying mice based on *Gps2* expression in brown adipose tissue (BAT) (**Figure S2D and**
135 **S2E-F**) or in liver (data not shown). Altogether, the data suggest that GPS2 action in WAT
136 may influence insulin secretion from beta cells in humans and in mice.

137

138 **Specific Depletion of GPS2 in Adipocytes Impacts Insulin Secretion upon Diet-Induced** 139 **Obesity**

140 To assess the impact of adipocyte GPS2 deficiency on the regulation of insulin secretion upon
141 diet-induced obesity, GPS2 AKO mice and their WT littermates were subjected to either
142 normal chow-diet (CD) or high-fat diet (HFD) for 4 and 12 weeks and then, glucose homeo-
143 stasis and insulin secretion were monitored. Depletion of GPS2 was efficient in WAT and
144 BAT depots in GPS2 AKO mice while GPS2 expression was not altered in liver and pancreat-
145 ic islets, as expected (**Figure S2G**). As previously described (Drareni et al., 2018; Fan et al.,
146 2016), GPS2 AKO mice were more glucose intolerant than WT controls after 4 weeks and 12
147 weeks of HFD, while no difference was observed in CD (**Figure S3A**). Fasting insulin con-
148 centration was lower (trend) in the blood of GPS2 AKO mice compared to WT mice only
149 under obese conditions (**Figure 2E**). In agreement with this observation, insulin secretion,
150 measured during the oral glucose tolerance test (OGTT), was altered in the GPS2 AKO mice
151 compared to WT mice after 4 weeks and 12 weeks of HFD, while no difference was observed
152 under CD conditions (**Figure 2F and Figure S3B-C**). Indeed, insulin secretion calculated
153 using the ratio between insulin concentrations at 15 min after glucose ingestion to baseline
154 was lower in the GPS2 AKO mice compared to WT mice upon HFD (**Figure 2G**).

155 Impaired insulin secretion by the pancreas in response to glucose can be the result of
156 decreased beta cell mass and/or impaired function of beta cells to produce insulin in response to
157 glucose (Dalmas, 2019b; Donath et al., 2013). In order to identify the mechanisms underlying
158 the inadequate insulin secretion caused by GPS2 deficiency in mature adipocytes, we evaluat-
159 ed the size and number of pancreatic islets in our mice (**Figures 3A-C**). We did not observe
160 significant changes in the number of islets in both genotypes under CD and HFD (**Figure 3B**
161 **and Figure S3D**). Unexpectedly, the islet size (surface) was significantly reduced in GPS2
162 AKO mice compare to WT only upon HFD (**Figures 3A-C**). The inadequate adaptation of
163 pancreatic islets to HFD could have been provoked by an increased local inflammation and
164 beta cell apoptosis (Dalmas, 2019a). In support of this possibility, we found that pancreatic
165 islets from GPS2 AKO mice exhibited increased macrophage infiltration and beta cell apop-
166 tosis in conjunction with decreased beta cell proliferation compared to WT mice under HFD
167 conditions, as assessed by Mac2+ staining, TUNEL assay, and Ki67+ staining, respectively
168 (**Figures 3D-H**). Inflammatory and apoptotic signaling molecules were also increased at the
169 mRNA level in pancreatic islets from HFD-fed GPS2 AKO mice compared to WT controls
170 (**Figures 3I and 3J**). Of note, proliferative markers were also deregulated in islets from HFD-
171 fed GPS2 AKO mice suggesting maladaptation to energy surplus (**Figure 3K**). We also ob-
172 served that expression of beta cell differentiation markers such as *Ins2*, *Mafb*, *Glut2*, *Nkx6-1*
173 and *Pdx-1* was reduced in islets of HFD-fed GPS2 AKO mice compared to WT mice (**Figure**
174 **3L**). Consistent with potential increased local inflammation, beta cell apoptosis and dediffer-
175 entiation, pancreatic islets isolated from HFD-fed GPS2 AKO mice secreted less insulin in
176 response to glucose stimulation than WT controls (**Figure 3M**).

177

178 **WAT Secretory Products from GPS2 AKO Mice Provoke Islet Dysfunction**

179 Above data suggested that beta cell mass and function is altered in obese GPS2 AKO mice.
180 We therefore considered that secreted factors from GPS2-deficient WAT depots may alter
181 islet function. To further investigate this adipocyte-islet crosstalk, isolated pancreatic islets
182 from healthy WT mice were incubated with medium from WAT or BAT explants or serum
183 from HFD-fed WT and GPS2 AKO mice for 24 h, followed by measurement of glucose-
184 stimulated insulin secretion (**Figures 4A and 4B**). We observed that islets incubated with
185 WAT explant medium or serum from GPS2 AKO mice were less potent in secreting insulin
186 than islets treated with WAT explant medium or serum from WT mice. Despite efficient
187 GPS2 depletion in the BAT of AKO mice, we did not observe any inhibitory effect of BAT
188 explant medium from AKO mice, as compared to medium from WT mice, on insulin secre-

189 tion (**Figure S4F**). Importantly, 1 h stimulation with WAT explant from GPS2 KO mice did
190 not alter insulin secretion in comparison to WAT explant from WT mice (data not shown).
191 This result suggests that WAT secretory products did not interfere with glucose-induced de-
192 polarization of the plasma membrane required for secretion of insulin. Islet dysfunction, me-
193 diated by medium from GPS2 AKO mice, was characterized by an increased expression of
194 inflammatory (*Emr1 (F4/80)*, *Il1- β* and *TNF- α*) and apoptotic (*Fas* and *Cas3*) genes (**Figure**
195 **4C**). Interestingly, the inhibitory signal from WAT explant medium or serum from GPS2
196 AKO mice was lost after heat-inactivating the medium or the serum (**Figure 4D**), suggesting
197 that secreted proteins and peptides (such as adipokines, cytokines and hormones) rather than
198 metabolites may link WAT dysfunction to impaired insulin secretion.

199 In order to characterize the GPS2-dependent gene signature in WAT depots that may contrib-
200 ute to beta cell dysfunction, we performed transcriptome analysis by RNA-sequencing and
201 RT-qPCR in 3 different WAT depots (subcutaneous (sc)WAT, epididymal (e)WAT, and mes-
202 enteric (mes)WAT). This analysis identified around 500 genes that were differentially ex-
203 pressed in all the 3 fat pads of GPS2 AKO mice, compared to WT mice, after 12 weeks of
204 HFD (**Figure 4E**). Gene ontology analysis revealed that the most up-regulated genes in
205 WATs of the GPS2 AKO mice are involved in immune responses and insulin signaling (**Fig-**
206 **ure 4E**), in agreement with our previous study (Drareni et al., 2018). This pathologic WAT
207 gene signature from GPS2 AKO mice was confirmed at the protein level in serum and WAT
208 explant media by measuring adipokines (adiponectin, leptin and resistin) and inflammatory
209 cytokines (IL6, TNFA, MCP-1/CCL2 and IL1B) (**Figures 4F and 4G**). Importantly, the BAT
210 of GPS2 AKO mice did not present the same phenotype as the WAT, which might explain the
211 lack of inhibitory capacity of BAT medium on insulin secretion (**Figure S4E**). Further,
212 mesWAT seemed to act differently from eWAT and scWAT, since the inhibitory effect on
213 islet function was not altered after heat inactivation, and the inflammatory profile of mesWAT
214 from GPS2 AKO mice was less pronounced than eWAT and scWAT (**Figures S4A and**
215 **S4B**). This difference is consistent with the proposed unique contribution of mesenteric fat, in
216 comparison to other WAT depots, in obesity complications (Dowal et al., 2017).

217

218

219 **DISCUSSION**

220

221 The pathogenesis of type 2 diabetes is a multifactorial disease involving interactions between
222 all metabolic tissues. Here we report that the dysfunction of white adipose tissue, driven by
223 the depletion of the transcriptional coregulator GPS2 in adipocytes, induces a pancreatic dys-
224 function reflected by the failure of beta cells to adapt to diet-induced obesity. We have previ-
225 ously shown that GPS2 AKO mice develop adipocyte hypertrophy and glucose intolerance
226 (Drareni et al., 2018). However, despite systemic glucose intolerance, AKO mice did not de-
227 velop systemic insulin resistance, suggesting that the pancreatic response to glucose was im-
228 paired. Our current study elucidates the underlying mechanism by demonstrating that adipo-
229 cyte dysfunction and reprogramming in AKO mice leads to a reduction of pancreatic islet size
230 and an impaired insulin secretion in response to glucose upon HFD (See Graphical Abstract).
231 Beta cell mass is characterized by its plasticity and its ability to adapt to different situations
232 such as pregnancy and weight gain (Golson et al., 2010; Sorenson and Brelje, 1997). In re-
233 sponse to HFD, beta cells produce more insulin, both by secreting more insulin per cell and
234 by increasing cell mass. Surprisingly, both mechanisms seem to be impaired in the GPS2
235 AKO mice islets in response to HFD. Treating pancreatic islets from C57BL6 WT mice with
236 adipose tissue-conditioned media from GPS2 AKO mice for 12 h was sufficient to inhibit
237 insulin secretion, while no effect was seen after 1 h. In addition to the defects in insulin secre-
238 tion, islets from GPS2 AKO mice also showed an increase of pro-apoptotic markers. Both
239 alterations could be the result of the exposure of the islets to pro-inflammatory cytokines
240 (IL1B, TNFA) and adipokines (leptin, resistin). It has been shown that short-time (12 to 48 h)
241 treatment of pancreatic beta cells with pro-inflammatory cytokines or adipokines results in
242 significant inhibition of insulin secretion (Cantley, 2014; Kiely et al., 2007; Ying et al., 2019;
243 Zhang and Kim, 1995). Furthermore, chronic exposure of beta cells to the same pro-
244 inflammatory cytokines and adipokines provokes increased inflammation and apoptosis re-
245 sulting in decreased islet size and function (Dalmas et al., 2017; Demine et al., 2020; Ying et
246 al., 2019).

247 Our results suggest that the pancreatic phenotype of GPS2 AKO mice is driven by mediators,
248 likely proteins and peptides, released by the dysfunctional and hypertrophic adipose tissue
249 from the AKO mice. This hypothesis is reinforced by the normal insulin secretion observed in
250 WT C57BL6 islets treated with a pre-heated adipose tissue-conditioned medium from GPS2
251 AKO mice. We believe that the phenotype of our GPS2 AKO mice is not due to one single
252 molecule but to the combination of several altered molecules, including inflammatory cyto-

253 kines and adipokines. In fact, a previous study from our laboratories demonstrated that mye-
254 loid deficiency of GPS2 provokes severe WAT inflammation without hypertrophy (Fan et al.,
255 2016), which is not characterized by alteration of insulin secretion but by an increase of insu-
256 lin production (adaptation to insulin resistance). These data suggest that inflammatory cyto-
257 kines, secreted from macrophages and/or adipocytes, are not the main mediators of the GPS2
258 AKO phenotype. Increased WAT inflammation in combination with deregulation of adi-
259 pokine secretion such as adiponectin, leptin and resistin as observed in WAT of GPS2 AKO
260 mice is more likely to be the main reason for a maladaptation of insulin secretion in GPS2
261 AKO upon HFD feeding.

262 Whereas WAT is well known to be characterized by a low-grade inflammation, increased
263 macrophage accumulation and pro-inflammatory cytokine and adipokine release during obesi-
264 ty, BAT in contrast seems to be more resistant to inflammation, as it displays less immune
265 cell infiltration and pro-inflammatory cytokine secretion than WAT (Dowal et al., 2017;
266 Fitzgibbons et al., 2011; Roberts-Toler et al., 2015). Specifically relevant for our study is the
267 notion that the infiltration of immune cells in the BAT begins only after 16 months of HFD in
268 mice (Dowal et al., 2017; Roberts-Toler et al., 2015), while GPS2 AKO mice were exposed to
269 HFD for either 4 or 12 weeks. Consistent with that, treating islets from WT mice with GPS2
270 AKO BAT conditioned media did not alter their insulin secretion after glucose stimulation.
271 Furthermore, GPS2 expression levels in the BAT of WT mice did not show any correlation
272 with their metabolic status (i.e, glucose tolerance and insulin sensitivity and secretion). There-
273 fore, our results support a mechanism in which the islet phenotype seen in GPS2 AKO mice is
274 governed by dysfunction and inflammation of the WAT but not the BAT.

275 While it seems clear that WAT dysfunction in GPS2 AKO mice and in humans with lower
276 GPS2 expression triggers pancreatic beta cell failure, there might be several mechanisms by
277 which the loss of GPS2 in adipocytes leads to that phenotype. However, the coincidence of
278 pancreatic dysfunction with adipocyte hypertrophy in the GPS2 AKO mice suggests that
279 these phenotypes are interconnected and the result of the same adipocyte reprogramming up-
280 on disruption of specific regulatory transcriptional networks. This is supported by other
281 mouse models of adipocyte hypertrophy, showing that the mice were glucose intolerant but
282 not insulin resistant, thus pointing at pancreatic dysfunction (Rohm et al., 2013). In our previ-
283 ous study (Drareni et al., 2018) we discovered that GPS2 represses the activity of the tran-
284 scription factor HIF1. Interestingly, adipocyte-specific overexpression of HIF1A is character-
285 ized by hypertrophic adipocytes, WAT insulin resistance and glucose intolerance (Halberg et
286 al., 2009). Despite the increased insulin resistant status of mice overexpressing HIF1A in adi-

287 pocytes, no change in glucose-induced insulin release was observed in comparison to control
288 mice, suggesting an inadequate adaptive response in pancreatic islets to produce insulin
289 (Halberg et al., 2009). By contrast, genetic or pharmacological inhibition of HIF1A in adipo-
290 cytes in obese mouse models is characterized by decreased adipose cell size, improvement of
291 glucose tolerance and insulin sensitivity, and a reduction of glucose-induced insulin release
292 (Jiang et al., 2011; Sun et al., 2013).The interplay between WAT phenotype, including hyper-
293 trophy, and islet remodeling upon obesity is further supported by very recent studies in hu-
294 mans ((Kusminski et al., 2020), Gao et al. 2020 preprint
295 <https://doi.org/10.1101/2020.06.12.148809>) Together, these studies emphasize a potentially
296 significant role of the GPS2 regulatory network in adipocytes for linking the WAT phenotype
297 to the regulation of adaptive islet responses upon energy surplus.

298

299 **ACKNOWLEDGEMENTS**

300 N.V. was supported by grants from the French National Agency of Research (PROVIDE and
301 PUMAS), the French and European Foundation for Diabetes (SFD and EFSD), and
302 the European Union H2020 framework (ERC-EpiFAT 725790). Human study was performed
303 at the Clinical Investigation Centre (Groupe Hospitalier Saint-Louis/Lariboisière, Paris) and
304 were supported by Assistance Publique des Hôpitaux de Paris (APHP; PHRC AOR09087; J.-
305 F.G., principal investigator [PI]). E.D was supported by grants from ATIP-
306 AVENIR, the French and European Foundation for Diabetes (SFD and EFSD). E.T. was sup-
307 ported by grants from the Swedish Research Council, the Swedish Diabetes Foundation,
308 the Novo Nordisk Foundation, and the Center for Innovative Medicine (CIMED) at the Ka-
309 rolinska Institutet. RNA sequencing and transcriptome analysis were supported by the France
310 Génomique national infrastructure, funded as part of the “Investissements d’Avenir” program
311 managed by the Agence Nationale de la Recherche (ANR-10-INBS-09).

312

313 **AUTHOR CONTRIBUTIONS**

314 KD and NV designed research studies, analyzed data, and wrote the manuscript. KD, FA, RB
315 conducted the in vivo experiments, acquired and analyzed data with the help of CC, SB, AG
316 and ED. RR, GV, JLN and JFG conducted human analysis and wrote the manuscript. KD and
317 SL conducted transcriptomic analyses. ET, ED, and FA helped in the experimental design,
318 data interpretation and manuscript writing.

319

320

321
322
323
324
325
326
327
328
329
330
331
332
333
334
335
336
337
338
339
340
341
342
343
344
345
346
347
348
349
350
351
352
353
354
355
356
357
358
359
360
361
362
363
364
365
366

STAR METHODS

- KEY RESSOURCES TABLE
- RESOURCE AVAILABILITY
 - Lead Contact,
 - Materials Availability
 - Data and Code Availability
- EXPERIMENTAL MODEL AND SUBJECT DETAILS
- METHODS DETAILS
 - In vivo treatments and metabolic measurements
 - Analysis of different metabolic circulating factors in explant medium
 - Histology, immunofluorescence and microscopy
 - Isolation of pancreatic islets from mice
 - Glucose-stimulated insulin secretion assay
 - Explants medium collection and islets treatment
 - RT-qPCR analysis
 - RNA sequencing and transcriptomic analysis
- QUANTIFICATION AND STATISTICAL ANALYSIS

367
368
369
370
371
372
373
374
375
376
377
378
379
380
381
382
383
384
385
386
387
388
389
390
391
392
393
394
395
396
397
398
399
400
401
402

RESOURCES AVAILABILITY

Lead Contact

Further information and requests for resources and reagents should be directed to and will be fulfilled by the Lead Contacts: Nicolas Venteclef (nicolas.venteclef@inserm.fr)

Material availability

This study did not generate new unique reagents.

Data and Code Availability

The RNA-Seq gene expression data and raw fastq files are available on the GEO repository: GSE111647 (www.ncbi.nlm.nih.gov/geo/).

EXPERIMENTAL MODEL AND SUBJECT DETAILS

Clinical study

Human population: Biopsies from subcutaneous adipose tissue (SAT) were obtained from participants admitted to the Lariboisière hospital, University centre of diabetes and its complications, Paris, France. Clinical and anthropometric data are summarized in **Table S1**. The study was conducted in accordance with the Helsinki Declaration and was registered in a public trial registry (Clinicaltrials.gov; NCT02368704). The Ethics Committee of CPP Ile-de-France approved the clinical investigations for all individuals, and written informed consent was obtained from all individuals. The principal investigator of this clinical trial is Prof. Gautier Jean-François: jean-francois.gautier@aphp.fr.

Measurement of insulin secretion: Insulin secretion was evaluated during the administration of graded infusions of glucose. Participants were instructed to eat a diet in which carbohydrates comprised at least 50% of total calories for at least five days preceding the test. Studies were started at 8:00-9:00 AM with subjects in the recumbent position after a 12h overnight fast. Intravenous catheters were placed in the right and in the left forearms for glucose administration and blood sampling. Following a 30 min baseline sampling period, a graded intravenous infusion of 30% glucose was then started at a rate of 2 mg/kg body weight.min⁻¹, followed by infusions at 4, 6, 8 and 10 mg/kg body weight.min⁻¹. Each infusion rate was maintained for a period of 40 min. Blood samples were drawn every 10 min throughout the experiment for measurement of glucose and C-peptide concentrations. *Measurement of acute insu-*

403 lin and glucagon secretions: At the end of the glucose ramping, the 20% glucose infusion rate
404 was adjusted to obtain a blood glucose level of approximately 400 mg/dL (22 mmol/L). Glu-
405 cose infusion was then maintained and an i.v. bolus of 5 g of arginine chlorhydrate was ad-
406 ministered in 45 seconds, with venous blood sample collection before and 2, 3, 4, 5, 10, and
407 15 minutes after the bolus for measurements of insulin, glucagon et C-peptide.

408 Data analysis: Relationships between glucose levels and pre-hepatic insulin secretion rates
409 (ISR) during graded intravenous glucose infusions were explored. ISR and glucose levels used
410 in the analysis represented the average of the values for each individual at each glucose infu-
411 sion rate step. ISR was then plotted against the corresponding glucose level to define a dose-
412 response relationship. ISR were derived by deconvolution of circulating C-peptide concentra-
413 tions (Eaton et al., 1980) using version 3.4a of the ISEC software (Hovorka, 1993). Individual
414 kinetics parameters of C-peptide clearance are computed by ISEC from standard kinetic pa-
415 rameters, taking into account the age, sex, body surface area, and glucose tolerance status of
416 the subject. The M index obtained during a hyperinsulinemic euglycemic clamp (data not
417 shown) was used as an index of insulin sensitivity.

418

419 **Animals**

420 *Gps2*^{flox/flox} mice were generated at Ozgene Pty, Ltd. (Bentley DC, Australia) using a targeting
421 construct, which contained loxP sites flanking exons 2 and 5, followed by a FRT site and a
422 neomycin cassette inserted between exons 5 and 6. The targeting vector was electroporated
423 into C57BL/6 Bruce4 embryonic stem (ES) cells. The correctly recombined ES colony was
424 then injected into C57BL/6 blastocysts. Male chimeras were mated with female C57BL/6
425 mice to get mice with a targeted *Gps2* allele. The mice were crossbred with C57BL/6 flp-
426 recombinase mice to remove the neomycin cassette to create heterozygous *Gps2*^{flox/+} mice.
427 The mice were then crossbred with C57BL/6 mice for nine generations before being bred with
428 heterozygous *Gps2*^{flox/+} mice to get the *Gps2*^{flox/flox} mice (Fan et al., 2016). To generate adipo-
429 cyte-specific *Gps2* KO mice, *Gps2*^{flox/flox} mice were crossed with adiponectin-*Cre* mice
430 (B6;FVB-Tg (Adipoq-*Cre*) 1Evdr/J; Jackson Laboratory stock no. 010803). KO mice were
431 bred for at least nine generations before the experiments were started. Adipoq-*Cre-Gps2*^{flox/flox}
432 littermates were used as control. All mice used in the studies were male, between 7–8 weeks
433 old at the time of the experiment starting point, and randomized before any experiment was
434 started. All animal experiments were approved by the French ethical board (Paris-Sorbonne
435 University, Charles Darwin N°5, 01026.02) and conducted in accordance with the guidelines

436 stated in the International Guiding Principles for Biomedical Research Involving Animals,
437 developed by the Council for International Organizations of Medical Sciences (CIOMS). All
438 mice strains were bred and maintained at the “Centre exploration fonctionnel (CEF)” at Paris
439 Sorbonne University (UMS_28).

440 METHODS DETAILS 441

442 ***In vivo* treatments, metabolic measurements**

443 Diet-induced obesity and insulin resistance

444 7–8-weeks-old WT and GPS2 AKO mice were fed with a 60%-fat diet (HFD, Research Diets,
445 D12492) for 4 and 12 weeks.

446 Oral glucose tolerance test (OGTT):

447 Mice were fasted overnight before receiving an oral gavage of glucose (2 g/kg). Blood glu-
448 cose levels were measured directly from tail vein blood at 0, 15, 30, 45, 60 and 90 min using a
449 glucometer (Accu-Chek Performa, Roche). Blood samples were taken from the tail vein at 0,
450 15, 30 and 60 min.

451

452 **Analysis of different metabolic circulating factors in explant medium**

453 Adiponectin, leptin, IL6, MCP-1, PA-1 and resistin concentrations were determined by using
454 MULTIPLEX Adipocyte kit according to the manufacturer’s instructions (Millipore,
455 MADCYMAG-72K).

456

457 **Histology, immunofluorescence and microscopy**

458 Pancreatic tissue samples were fixed in 10% formaldehyde solution overnight and embedded
459 in paraffin. For beta cell area analysis, epitope-specific antibody was used for IF detection of
460 insulin (Cell Signaling Technology, 1:200). For macrophages infiltration detection, specific
461 Mac2 antibody was used (Cell Signaling Technology 1:200). For IF analysis, cleared and re-
462 hydrated sections were quenched with 3% H₂O₂ for 15 min at room temperature then washed
463 twice for 5 min each with TBS + 0.1 % (vol/vol) Tween-20. Sections were then blocked with
464 TBS + 3 % (vol/vol) BSA for 30 min at room temperature. Sections were then incubated for
465 one hour at room temperature or overnight at 4°C with diluted primary antibodies, washed 3
466 times for 5 min with TBS + 0.1 % (vol/vol) Tween-20, followed by incubation with appropri-
467 ate fluorophore-conjugated secondary antibodies (Invitrogen). Sections were then washed
468 twice for 5 min with TBS then mounted with hard-set DAPI-containing mounting media

469 (Vectashield, Vector Labs). Images were acquired on an Axiovert 200M microscope or
470 through whole slide scanning with ZEISS AxioScan.

471 Mac2⁺ cells and TUNEL⁺ cells were quantified based on the average number of
472 Mac2⁺/TUNEL⁺ cells per islets in all islets identified in histological sections collected from
473 WT and AKO mice. Ki67⁺ cells was quantified based on the average number of Ki67⁺ Insu-
474 lin⁺ cells per islets (normalized by the islets area) in all islets identified in histological sec-
475 tions collected from WT and AKO mice.

476

477 **Isolation of pancreatic islets from mice**

478 To isolate islets, pancreas was perfused through the common bile duct with a HBSS colla-
479 genase solution (1.4 g/L; collagenase type 4 Worthington) and digested in the same solution
480 in a 37°C water bath for 15-18 min as previously described (Dalmas et al., 2017). After shak-
481 ing for 15 seconds, pancreas were washed three times with HBSS supplemented with 0.5%
482 bovine serum albumin (BSA) and filtrated through 500 mm and 70 mm cell strainers (Corn-
483 ing). Islets were retained on the 70 mm cell strainer while the cell mixture passing through the
484 70 mm cell strainer represented the exocrine stoma. Islets from the same condition were dou-
485 ble handpicked and pooled into a Petri dish with RPMI-1640 (GIBCO) containing 11.1 mM
486 glucose, 100 units/ml penicillin, 100 mg/ml streptomycin, 2 mM Glutamax, 50 mg/ml gen-
487 tamycin, 10 mg/ml Fungison and 10% FCS (Invitrogen). Islets were used directly for RNA
488 isolation or cell culture in humid environment containing 5% CO₂.

489

490 **Glucose-stimulated insulin secretion assay**

491 Islets were seeded in 60 mm culture dishes for 24 h in RPMI-1640 containing mouse islet
492 medium. 25 islets were transferred to 35 mm culture dishes and then pre-incubated for 1 h in
493 modified Krebs-Ringer bicarbonate buffer (KRB; 115 mM NaCl, 4.7 mM KCl, 2.6 mM
494 CaCl₂ 2H₂O, 1.2 mM KH₂PO₄, 1.2 mM MgSO₄ 7H₂O, 10 mM HEPES, 0.5% BSA [pH 7.4])
495 with no glucose, KRB was then replaced by KRB 2.8 mM glucose for 2 h (basal insulin re-
496 lease) or by 2 h in KRB (16.7 mM glucose) (stimulated insulin release). Insulin content was
497 harvested by extraction with 0.18 N HCl in 70% EtOH. Insulin concentrations were deter-
498 mined using a mouse insulin ultrasensitive mouse/rat insulin kit (Meso Scale Discovery,
499 Rockville, MD, USA).

500

501 **Explants medium collection and islets treatment**

502 Pieces eWAT, scWAT and MesWat pads and liver were isolated from mice and sliced into
503 equally sized pieces of 50-100ug. Explants were washed twice in PBS and cultured in ECBM
504 (endothelial cell basal medium) supplemented with 1% svf and 1% PS for the fat pads and
505 Williams Medium E for liver supplemented with 1% svf and 1% PS during 24H. Islets from
506 C57BL6/J mice were isolated (as previously described) and treated with explant medium di-
507 luted 1:8 during 12H.

508

509 **RT-qPCR analysis**

510 RNA was extracted from tissues or purified cells using the RNeasy RNA Mini Kit (Qiagen).
511 Complementary DNAs were synthesized using M-MLV Reverse Transcriptase kit (Promega)
512 for the adipose tissue and using super script kit (Promega) for the islets. RT-qPCR was per-
513 formed using the QuantStudio 3 Real-Time PCR Systems (ThermoFisher Scientific). 18S was
514 used for normalization to quantify relative mRNA expression levels. Relative changes in
515 mRNA expression were calculated using the comparative cycle method ($2^{-\Delta\Delta Ct}$).

516

517 **RNA-sequencing analyses**

518 Library preparation and Illumina sequencing were performed at the Ecole normale superieure
519 genomic core facility (Paris, France). Messenger (polyA+) RNAs were purified from 400 µg
520 of total RNA using oligo(dT). Libraries were prepared using the strand specific RNA-Seq
521 library preparation TruSeq Stranded mRNA kit (Illumina). Libraries were multiplexed by 12
522 on 2 runs. A 75 bp single read sequencing was performed on a NextSeq 500 (Illumina). A
523 mean of $25,44 \pm 6,01$ million passing Illumina quality filter reads was obtained for each of the
524 12 samples. The analyses were performed using the Eoulsan pipeline (Jourden et al., 2012),
525 including read filtering, mapping, alignment filtering, read quantification, normalization and
526 differential analysis: Before mapping, poly N read tails were trimmed, reads ≤ 40 bases were
527 removed, and reads with quality mean ≤ 30 were discarded. Reads were then aligned against
528 the *Mus musculus* genome from Ensembl version91 using STAR (version 2.6.1b) (Dobin et
529 al., 2013). Alignments from reads matching more than once on the reference genome were
530 removed using Java version of samtools (Li et al., 2009). To compute gene expression, *Mus*
531 *musculus* GTF genome annotation version 91 from Ensembl database was used. All overlap-
532 ping regions between alignments and referenced exons were counted using HTSeq-count
533 0.5.3 (Anders et al., 2015). The sample counts were normalized using DESeq2 1.8.1 (Love et
534 al., 2014). Statistical treatments and differential analyses were also performed using DESeq2
535 1.8.1. Mouse individuals, sampled tissues and mouse genotypes were taken into account in

536 the DESeq2 as well as the interaction between individuals, genotype and tissues.

537

538 **QUANTIFICATION AND STATISTICAL ANALYSIS**

539

540 Human data are expressed as mean \pm SD or as mean \pm SEM as indicated in the text, tables
541 and figures. Analyses of variance (ANOVA) or covariance (ANCOVA) were used for group
542 comparisons. Repeated measures analyses of variance (MANOVA) were employed to com-
543 pare glucose, insulin and C-peptide values across a period of time during the graded intrave-
544 nous infusions of glucose. Mixed regression model with random effects was employed to
545 compare glucose/ISR response curves. Mouse data are expressed as mean \pm SEM. Experi-
546 ments were performed at least 3 times. Student's *t* test and ANOVA were employed for com-
547 parisons between groups. Statistics were performed with JMP (SAS Institute Inc, Cary, NC)
548 or with GraphPad software (Prism). $P \leq 0.05$ is significant.

549 $\left[\begin{array}{l} \text{L} \\ \text{SEP} \end{array} \right]$

550

551

552 **REFERENCES**

- 553 Anders, S., Pyl, P.T., and Huber, W. (2015). HTSeq--a Python framework to work with
554 high-throughput sequencing data. *Bioinformatics* 31, 166-169.
- 555
556 Cantley, J. (2014). The control of insulin secretion by adipokines: current evidence for
557 adipocyte-beta cell endocrine signalling in metabolic homeostasis. *Mammalian genome :
558 official journal of the International Mammalian Genome Society* 25, 442-454.
- 559
560 Cardamone, M.D., Kronen, A., Tanasa, B., Taylor, H., Ricci, L., Ohgi, K.A., Glass, C.K.,
561 Rosenfeld, M.G., and Perissi, V. (2012). A protective strategy against hyperinflammatory
562 responses requiring the nontranscriptional actions of GPS2. *Molecular cell* 46, 91-104.
- 563
564 Cardamone, M.D., Tanasa, B., Cederquist, C.T., Huang, J., Mahdaviani, K., Li, W., Rosenfeld,
565 M.G., Liesa, M., and Perissi, V. (2018). Mitochondrial Retrograde Signaling in Mammals Is
566 Mediated by the Transcriptional Cofactor GPS2 via Direct Mitochondria-to-Nucleus
567 Translocation. *Molecular cell* 69, 757-772 e757.
- 568
569 Cardamone, M.D., Tanasa, B., Chan, M., Cederquist, C.T., Andricovich, J., Rosenfeld, M.G.,
570 and Perissi, V. (2014). GPS2/KDM4A pioneering activity regulates promoter-specific
571 recruitment of PPARgamma. *Cell Rep* 8, 163-176.
- 572
573 Cederquist, C.T., Lentucci, C., Martinez-Calejman, C., Hayashi, V., Orofino, J., Guertin, D.,
574 Fried, S.K., Lee, M.J., Cardamone, M.D., and Perissi, V. (2017). Systemic insulin sensitivity
575 is regulated by GPS2 inhibition of AKT ubiquitination and activation in adipose tissue.
576 *Molecular metabolism* 6, 125-137.
- 577
578 Dalmas, E. (2019a). Innate immune priming of insulin secretion. *Current opinion in
579 immunology* 56, 44-49.
- 580
581 Dalmas, E. (2019b). Role of innate immune cells in metabolism: from physiology to type
582 2 diabetes. *Seminars in immunopathology* 41, 531-545.
- 583
584 Dalmas, E., Lehmann, F.M., Dror, E., Wueest, S., Thienel, C., Borsigova, M., Stawiski, M.,
585 Traunecker, E., Lucchini, F.C., Dapito, D.H., et al. (2017). Interleukin-33-Activated Islet-
586 Resident Innate Lymphoid Cells Promote Insulin Secretion through Myeloid Cell
587 Retinoic Acid Production. *Immunity* 47, 928-942 e927.
- 588
589 Demine, S., Schiavo, A.A., Marin-Canas, S., Marchetti, P., Cnop, M., and Eizirik, D.L. (2020).
590 Pro-inflammatory cytokines induce cell death, inflammatory responses, and
591 endoplasmic reticulum stress in human iPSC-derived beta cells. *Stem cell research &
592 therapy* 11, 7.
- 593
594 Dobin, A., Davis, C.A., Schlesinger, F., Drenkow, J., Zaleski, C., Jha, S., Batut, P., Chaisson,
595 M., and Gingeras, T.R. (2013). STAR: ultrafast universal RNA-seq aligner. *Bioinformatics*
596 29, 15-21.
- 597
598 Donath, M.Y., Dalmas, E., Sauter, N.S., and Boni-Schnetzler, M. (2013). Inflammation in
599 obesity and diabetes: islet dysfunction and therapeutic opportunity. *Cell metabolism* 17,
600 860-872.

601 Dowal, L., Parameswaran, P., Phat, S., Akella, S., Majumdar, I.D., Ranjan, J., Shah, C., Mogre,
602 S., Guntur, K., Thapa, K., et al. (2017). Intrinsic Properties of Brown and White
603 Adipocytes Have Differential Effects on Macrophage Inflammatory Responses. *Mediators
604 of inflammation* 2017, 9067049.
605
606 Drareni, K., Ballaire, R., Barilla, S., Mathew, M.J., Toubal, A., Fan, R., Liang, N., Chollet, C.,
607 Huang, Z., Kondili, M., et al. (2018). GPS2 Deficiency Triggers Maladaptive White Adipose
608 Tissue Expansion in Obesity via HIF1A Activation. *Cell Rep* 24, 2957-2971 e2956.
609
610 Eaton, R.P., Allen, R.C., Schade, D.S., Erickson, K.M., and Standefer, J. (1980). Prehepatic
611 insulin production in man: kinetic analysis using peripheral connecting peptide
612 behavior. *J. Clin. Endocrinol. Metab.* 51, 520-528.
613
614 Fan, R., Toubal, A., Goni, S., Drareni, K., Huang, Z., Alzaid, F., Ballaire, R., Ancel, P., Liang,
615 N., Damdimopoulos, A., et al. (2016). Loss of the co-repressor GPS2 sensitizes
616 macrophage activation upon metabolic stress induced by obesity and type 2 diabetes.
617 *Nat Med* 22, 780-791.
618
619 Fitzgibbons, T.P., Kogan, S., Aouadi, M., Hendricks, G.M., Straubhaar, J., and Czech, M.P.
620 (2011). Similarity of mouse perivascular and brown adipose tissues and their resistance
621 to diet-induced inflammation. *American journal of physiology. Heart and circulatory
622 physiology* 301, H1425-1437.
623
624 Golson, M.L., Misfeldt, A.A., Kopsombut, U.G., Petersen, C.P., and Gannon, M. (2010). High
625 Fat Diet Regulation of beta-Cell Proliferation and beta-Cell Mass. *The open
626 endocrinology journal* 4.
627
628 Halberg, N., Khan, T., Trujillo, M.E., Wernstedt-Asterholm, I., Attie, A.D., Sherwani, S.,
629 Wang, Z.V., Landskroner-Eiger, S., Dineen, S., Magalang, U.J., et al. (2009). Hypoxia-
630 inducible factor 1alpha induces fibrosis and insulin resistance in white adipose tissue.
631 *Molecular and cellular biology* 29, 4467-4483.
632
633 Hovorka, R. (1993). A computer program to reconstruct insulin secretion. *Diabetologia*
634 36 (suppl.1), A68.
635
636 Jiang, C., Qu, A., Matsubara, T., Chanturiya, T., Jou, W., Gavrilova, O., Shah, Y.M., and
637 Gonzalez, F.J. (2011). Disruption of hypoxia-inducible factor 1 in adipocytes improves
638 insulin sensitivity and decreases adiposity in high-fat diet-fed mice. *Diabetes* 60, 2484-
639 2495.
640
641 Jourdain, L., Bernard, M., Dillies, M.A., and Le Crom, S. (2012). Eoulsan: a cloud
642 computing-based framework facilitating high throughput sequencing analyses.
643 *Bioinformatics* 28, 1542-1543.
644
645 Kiely, A., McClenaghan, N.H., Flatt, P.R., and Newsholme, P. (2007). Pro-inflammatory
646 cytokines increase glucose, alanine and triacylglycerol utilization but inhibit insulin
647 secretion in a clonal pancreatic beta-cell line. *The Journal of endocrinology* 195, 113-
648 123.
649

650 Kita, S., Maeda, N., and Shimomura, I. (2019). Interorgan communication by exosomes,
651 adipose tissue, and adiponectin in metabolic syndrome. *J Clin Invest* 129, 4041-4049.
652

653 Kusminski, C.M., Ghaben, A.L., Morley, T.S., Samms, R.J., Adams, A.C., An, Y., Johnson, J.A.,
654 Joffin, N., Onodera, T., Crewe, C., et al. (2020). A Novel Model of Diabetic Complications:
655 Adipocyte Mitochondrial Dysfunction Triggers Massive beta-Cell Hyperplasia. *Diabetes*
656 69, 313-330.
657

658 Li, H., Handsaker, B., Wysoker, A., Fennell, T., Ruan, J., Homer, N., Marth, G., Abecasis, G.,
659 Durbin, R., and Genome Project Data Processing, S. (2009). The Sequence
660 Alignment/Map format and SAMtools. *Bioinformatics* 25, 2078-2079.
661

662 Love, M.I., Huber, W., and Anders, S. (2014). Moderated estimation of fold change and
663 dispersion for RNA-seq data with DESeq2. *Genome biology* 15, 550.
664

665 Marcelin, G., Silveira, A.L.M., Martins, L.B., Ferreira, A.V., and Clement, K. (2019).
666 Deciphering the cellular interplays underlying obesity-induced adipose tissue fibrosis. *J*
667 *Clin Invest* 129, 4032-4040.
668

669 Muir, L.A., Neeley, C.K., Meyer, K.A., Baker, N.A., Brosius, A.M., Washabaugh, A.R., Varban,
670 O.A., Finks, J.F., Zamarron, B.F., Flesher, C.G., et al. (2016). Adipose tissue fibrosis,
671 hypertrophy, and hyperplasia: Correlations with diabetes in human obesity. *Obesity*
672 (Silver Spring) 24, 597-605.
673

674 Roberts-Toler, C., O'Neill, B.T., and Cypess, A.M. (2015). Diet-induced obesity causes
675 insulin resistance in mouse brown adipose tissue. *Obesity* (Silver Spring) 23, 1765-1770.
676

677 Rohm, M., Sommerfeld, A., Strzoda, D., Jones, A., Sijmonsma, T.P., Rudofsky, G., Wolfrum,
678 C., Sticht, C., Gretz, N., Zeyda, M., et al. (2013). Transcriptional cofactor TBLR1 controls
679 lipid mobilization in white adipose tissue. *Cell metabolism* 17, 575-585.
680

681 Romacho, T., Elsen, M., Rohrborn, D., and Eckel, J. (2014). Adipose tissue and its role in
682 organ crosstalk. *Acta physiologica* 210, 733-753.
683

684 Scharfmann, R., Staels, W., and Albagli, O. (2019). The supply chain of human pancreatic
685 beta cell lines. *J Clin Invest* 129, 3511-3520.
686

687 Sorenson, R.L., and Brelje, T.C. (1997). Adaptation of islets of Langerhans to pregnancy:
688 beta-cell growth, enhanced insulin secretion and the role of lactogenic hormones.
689 *Hormone and metabolic research = Hormon- und Stoffwechselforschung = Hormones et*
690 *metabolisme* 29, 301-307.
691

692 Sun, K., Halberg, N., Khan, M., Magalang, U.J., and Scherer, P.E. (2013). Selective inhibition
693 of hypoxia-inducible factor 1alpha ameliorates adipose tissue dysfunction. *Molecular*
694 *and cellular biology* 33, 904-917.
695

696 Toubal, A., Clement, K., Fan, R., Ancel, P., Pelloux, V., Rouault, C., Veyrie, N., Hartemann, A.,
697 Treuter, E., and Venteclef, N. (2013). SMRT-GPS2 corepressor pathway dysregulation
698 coincides with obesity-linked adipocyte inflammation. *J Clin Invest* 123, 362-379.

699
700 Treuter, E., Fan, R., Huang, Z., Jakobsson, T., and Venticlef, N. (2017). Transcriptional
701 repression in macrophages-basic mechanisms and alterations in metabolic
702 inflammatory diseases. *FEBS letters* 591, 2959-2977.

703
704 Ying, W., Lee, Y.S., Dong, Y., Seidman, J.S., Yang, M., Isaac, R., Seo, J.B., Yang, B.H., Wollam,
705 J., Riopel, M., et al. (2019). Expansion of Islet-Resident Macrophages Leads to
706 Inflammation Affecting beta Cell Proliferation and Function in Obesity. *Cell metabolism*
707 29, 457-474 e455.

708
709 Zhang, S., and Kim, K.H. (1995). TNF-alpha inhibits glucose-induced insulin secretion in
710 a pancreatic beta-cell line (INS-1). *FEBS letters* 377, 237-239.

711
712

713 **DECLARATION OF INTERESTS**

714

715 There are no competing interests

716

717 **FIGURE LEGENDS**

718

719 **Figure 1: GPS2 expression level in WAT influences insulin secretion rate in humans.**

720 (A) Insulin secretion rate (ISR) by capillary blood glucose during a graded glucose infusion.
721 Participants were stratified by GPS2 mRNA expression as low or high expression as per val-
722 ues below (n=12) or above the median (n=11), respectively. Data are expressed as mean \pm
723 SEM. Statistics computed in a mixed regression model with random effects, and adjusted for
724 sex, age, insulin sensitivity index (M) and glycemic status. $p < 0.05$ is significant. Symbols
725 represent mean \pm SEM at baseline and at each glucose infusion step for Low or High expres-
726 sion groups of participants. For each participant, the average value of the four samples ob-
727 tained at 10 min intervals at each glucose infusion step were used. Curves represent a log-fit.
728 $p < 0.05$ is significant. (B) Leverage plot for the correlation between average insulin secretion
729 rate (ISR) (time 10 to 200 min) during a graded glucose infusion and GPS2 mRNA expres-
730 sion. Symbols represent data from individual participants. Correlation adjusted for sex, age,
731 baseline C-peptide and insulin sensitivity index (M) in a multiple regression analyses
732 $R^2 = 0.34$, $p = 0.004$ for ISR and GPS2 mRNA expression correlation, and $R^2 = 0.56$, $p = 0.0003$
733 for the whole model. (C) Correlation of Acute Insulin Response (AIR) during a glucose de-
734 pendent arginine stimulation and adipocyte GPS2 mRNA expression in multivariate analyses.
735 Correlation adjusted for sex, age, glycemic status (T2DM or ND), and pre-arginine injection
736 glucose levels. $R^2 = 0.31$, $p = 0.03$ for AIR and GPS2 mRNA $R^2 = 0.80$, $p < 0.0001$ for the whole
737 model. Acute Insulin Response defined as the mean of the 3 higher values from time 2 to 5
738 min.

739

740 **Figure 2: Adipocyte-specific GPS2 deficiency in mice leads to an impaired insulin secre-**
741 **tion in response to glucose.**

742 (A) RT-qPCR analysis of *GPS2* in eWAT from WT C57BL6/J under HFD-feeding for 12
743 weeks (n=18), classified into 2 groups: high GPS2 expression (n=9) and low GPS2 expression
744 (n=9). (B) Oral Glucose Tolerance Test (OGTT) in WT C57BL6 after 12 weeks of HFD clas-
745 sified into 2 groups: high GPS2 expression (n=9) and low GPS2 expression (n=9). (C) Meas-
746 urements of insulin secretion during the Oral Glucose Tolerance Test in WT C57BL6/J after
747 12 weeks of HFD classified into 2 groups: high GPS2 expression and low GPS2 expression
748 (high GPS2 n= 9 and low GPS2 n=9). (D) Glucose stimulated insulin secretion calculated
749 using the ratio of insulin secretion during OGTT at 15 min (T15) to basal (T0) in WT
750 C57BL6/J after 12 weeks of (HFD classified into 2 groups: high GPS2 expression and Low

751 GPS2 expression (high GPS2 n= 9 and low GPS2 n=9). (E) Fasting insulin concentration in
752 WT and GPS2 AKO mice in 4 and 12 weeks of HFD (n=5-6). (F) Measurements of insulin
753 secretion during the Oral Glucose Tolerance Test in WT and GPS2 AKO mice in 4 and 12
754 weeks of HFD (4 weeks HFD n=6, 12 weeks HFD n= 5-6). (G) Glucose stimulated insulin
755 secretion calculated using the ratio of insulin secretion during OGTT at 15 min (T15) to basal
756 (T0) in WT and GPS2 AKO mice in 4 and 12 weeks of HFD (4 weeks HFD n=6, 12 weeks
757 HFD n= 5-6). All data are represented as mean \pm S.E.M. *P <0.05, ** P <0.01, *** P <0.001.
758

759 **Figure 3: GPS2-deficiency in adipocytes provokes pancreatic islet inflammation and**
760 **beta cells apoptosis.**

761 (A) Representative images of insulin immunofluorescence staining in pancreas from WT and
762 GPS2 AKO mice in 4 and 12 weeks of HFD (4 weeks HFD n=6, 12 weeks HFD n= 6). (B-C)
763 Measurements of islets number (B) and surface (C) in pancreas from WT and GPS2 AKO
764 mice in 4 and 12 weeks of (4 weeks HFD n=6, 12 weeks HFD n= 6). (D) Representative im-
765 ages of Mac2 immunofluorescence staining in pancreas from WT and GPS2 AKO mice in 4
766 and 12 weeks of HFD (4 weeks HFD n=5, 12 weeks HFD n= 5). (E) Quantification of Mac2
767 positive cells in pancreatic islets from WT and GPS2 AKO mice in on HFD (4 weeks HFD
768 n=5, 12 weeks HFD n= 5). (F) Representative images of TUNEL+ immunofluorescence stain-
769 ing in pancreas from WT and GPS2 AKO mice on HFD (n=3). (G) Quantification of TUNEL
770 positive cells in pancreatic islets from WT and GPS2 AKO mice in 12 weeks of HFD (n=3).
771 (H) Representative images of Ki67+Insulin+ immunofluorescence staining and quantification
772 in pancreas from WT and GPS2 AKO mice fed with a HFD. (I- L) Measurement of inflam-
773 matory, apoptotic, proliferative and differentiation genes by RT-qPCR in pancreatic islets
774 from WT and GPS2 AKO mice after 12 weeks of HFD (n=3-5). (M) Glucose Stimulated In-
775 sulin Secretion (GSIS) of islets from WT and GPS2 AKO mice after 4 weeks of HFD treated
776 with low glucose (Low Glc, 2.8 mM) and high glucose (High Glc, 16.7 mM) (n=5). Results
777 are expressed as % of insulin content. All data are represented as mean \pm S.E.M. *P <0.05, **
778 P <0.01, *** P <0.001.

779

780 **Figure 4: The WAT secretome of GPS2 AKO mice promotes beta cell failure.**

781 (A-B) Glucose Stimulated Insulin Secretion (GSIS) of islets from WT C57BL6/J mice cul-
782 tured with scWAT, eWAT, mesWAT explant media or serum and treated with low glucose
783 (Low Glc, 2.8 mM) and high glucose (High Glc, 16.7 mM). Results are expressed in % of in-
784 sulin content (n=3). (C) Expression of inflammatory and apoptotic genes in isolated islets

785 from WT C57BL6/J mice cultured with eWAT explant media for 12h (n=3). (D) Glucose
786 Stimulated Insulin Secretion (GSIS) of islets from WT C57BL6/J mice cultured with scWAT,
787 eWAT and serum heat inactivated culture medium for 12h, then treated for 2h with low glu-
788 cose (Low Glc, 2.8 mM) and high glucose (High Glc, 16.7 mM). Results are expressed in %
789 of insulin content (n=3). (E) Transcriptome analyses by RNA sequencing of scWAT, epi-
790 WAT and mesWAT from WT and GPS2 AKO mice after 12 weeks of HFD (n=3). HeatMap
791 and Gene Ontology terms of the differentially expressed genes in WT and GPS2 AKO fat
792 pads. (F-G) WAT gene expression and secretome analysis of scWAT and eWAT from WT
793 and GPS2 AKO mice after 12 weeks of HFD (n=4-5). All data are represented as mean \pm
794 S.E.M. *P <0.05, ** P <0.01, *** P <0.001.

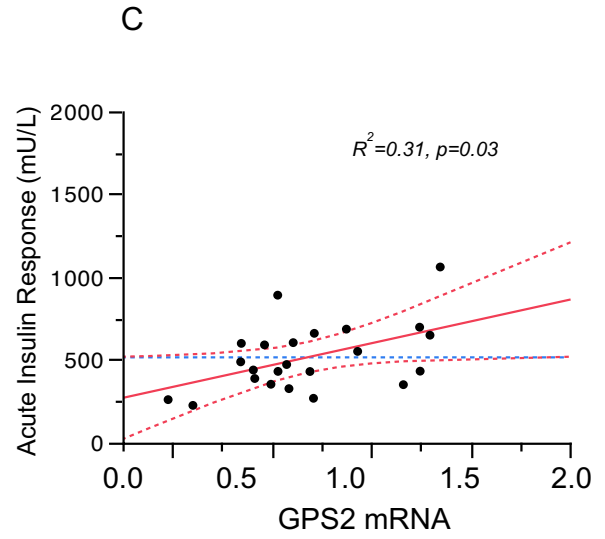
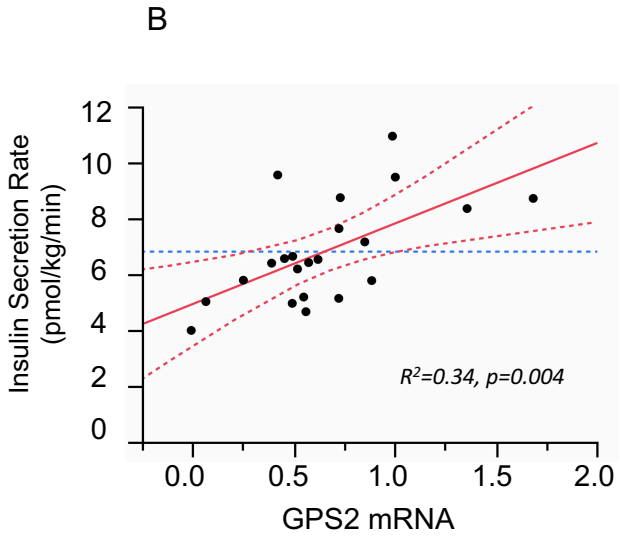
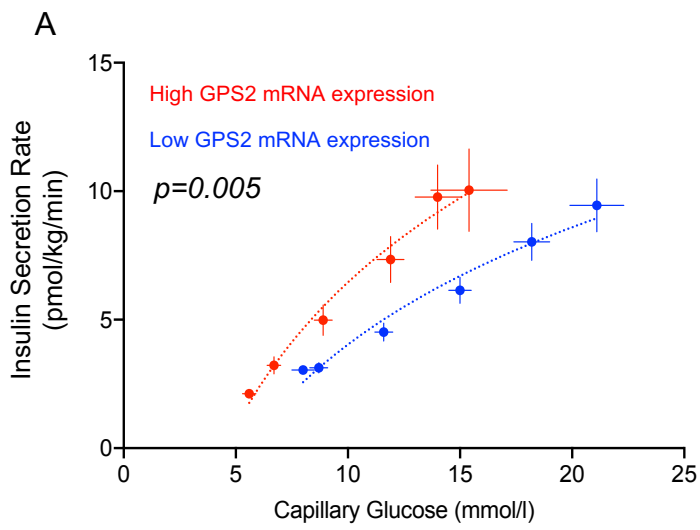


Figure 1

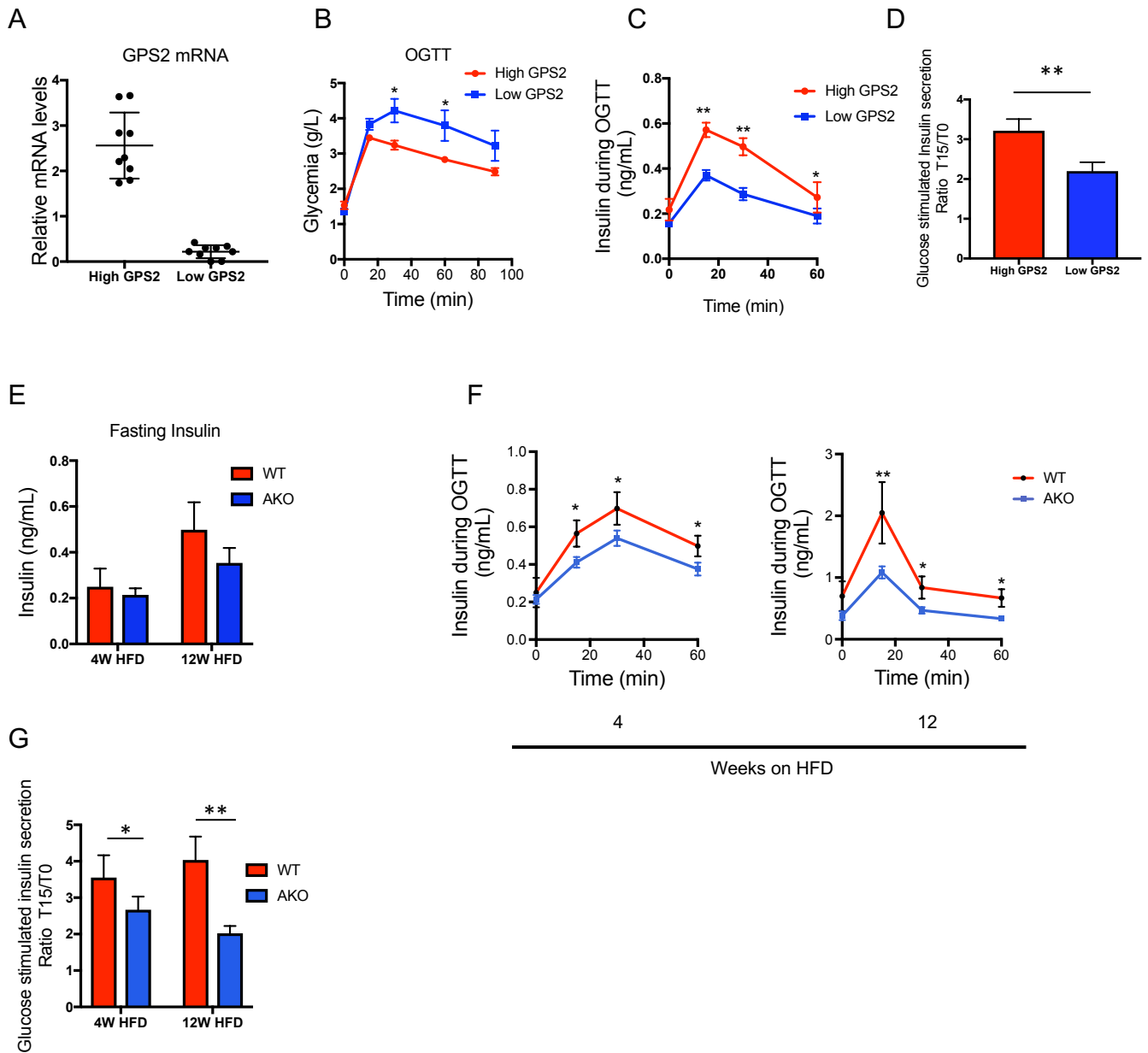


Figure 2

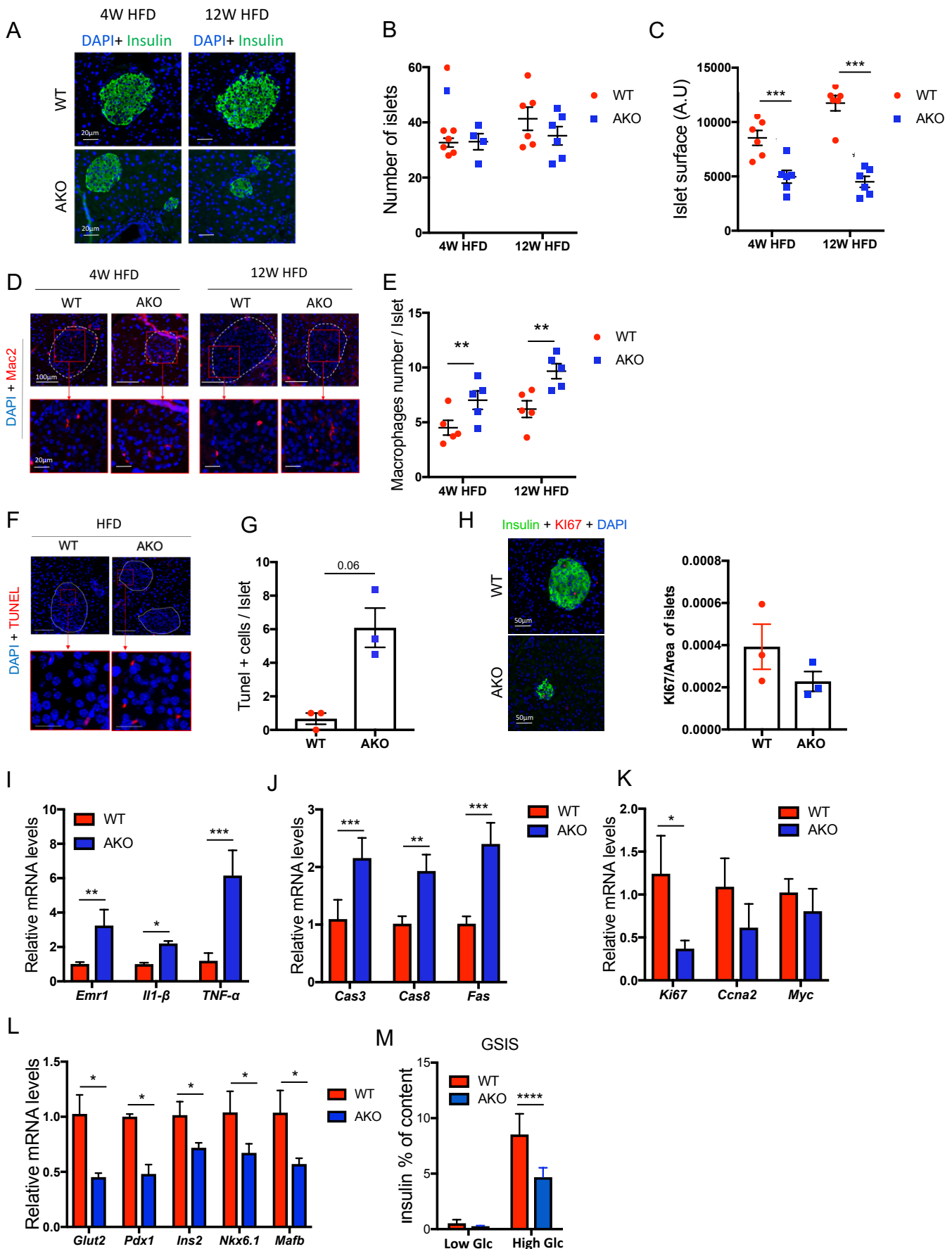


Figure 3

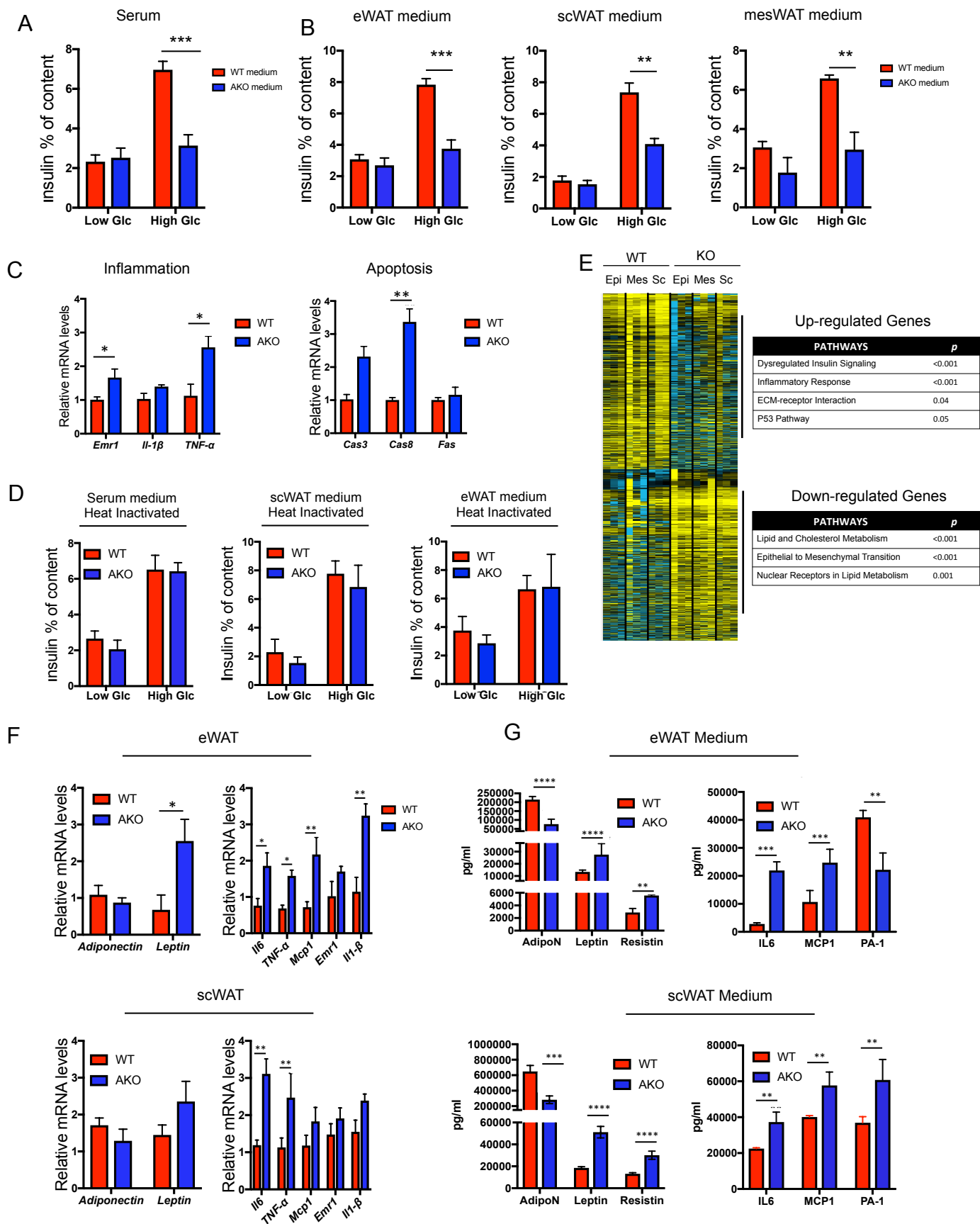
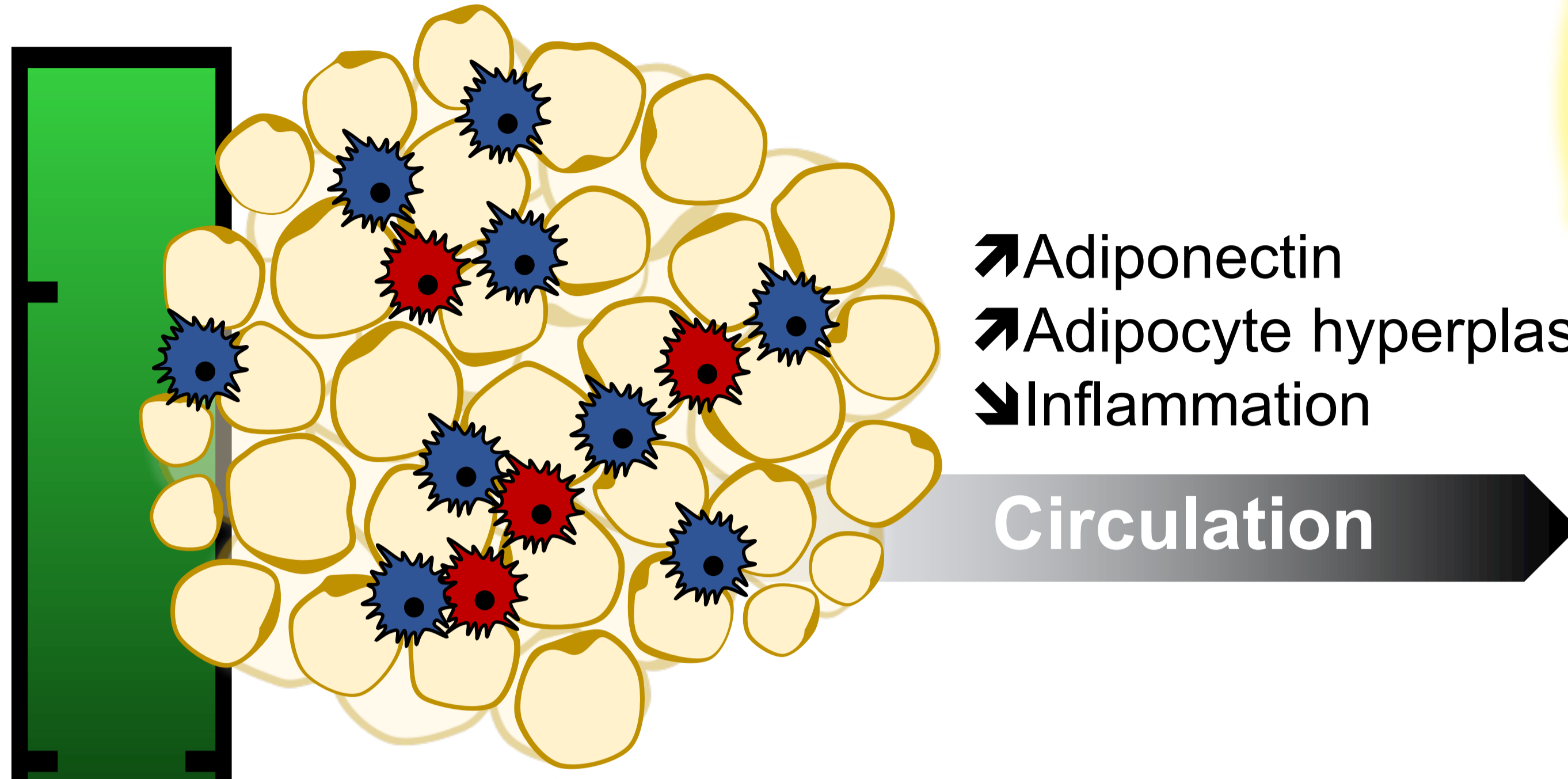


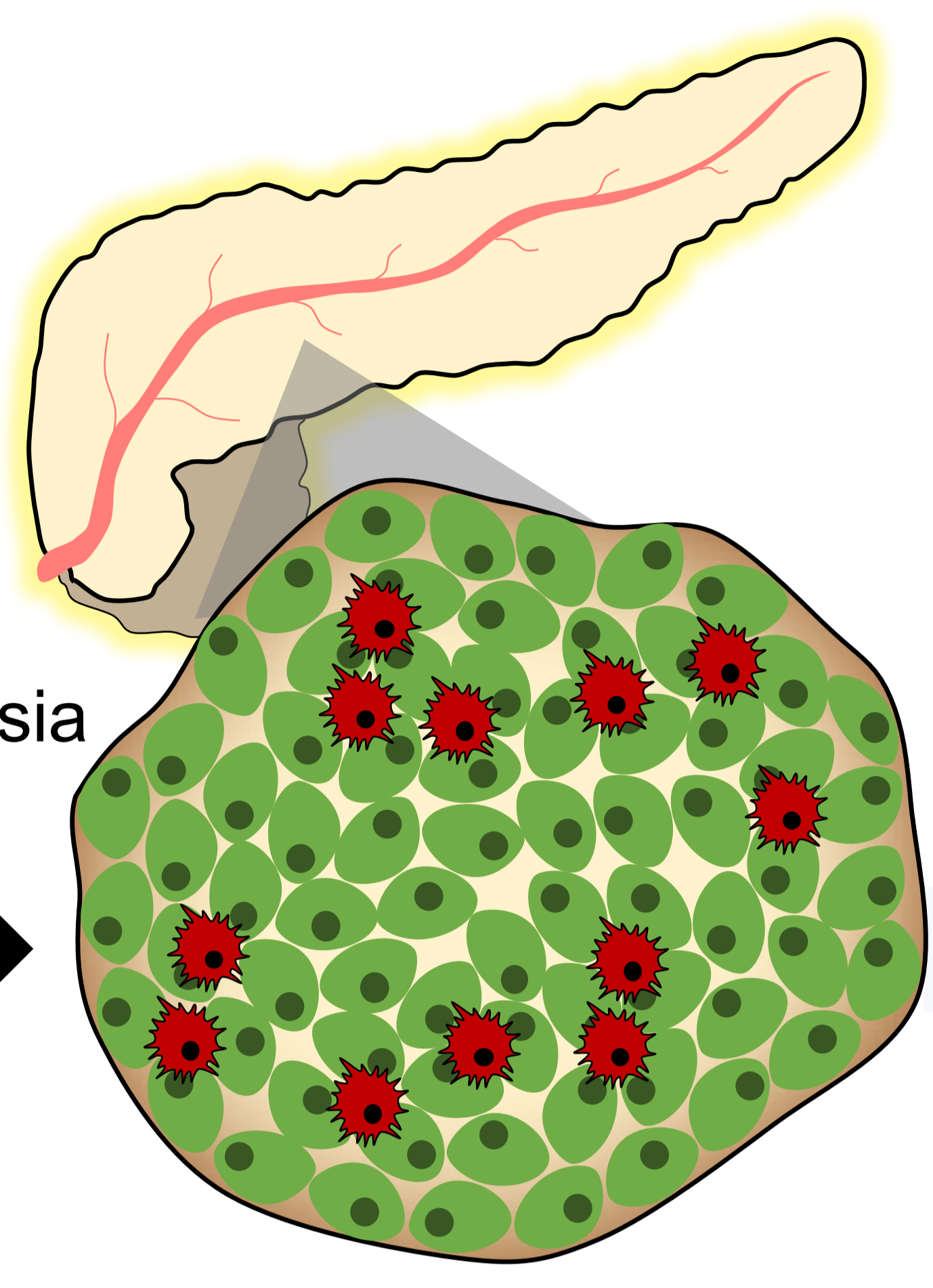
Figure 4

GPS2^{Hi}



- ↗ Adiponectin
- ↗ Adipocyte hyperplasia
- ↘ Inflammation

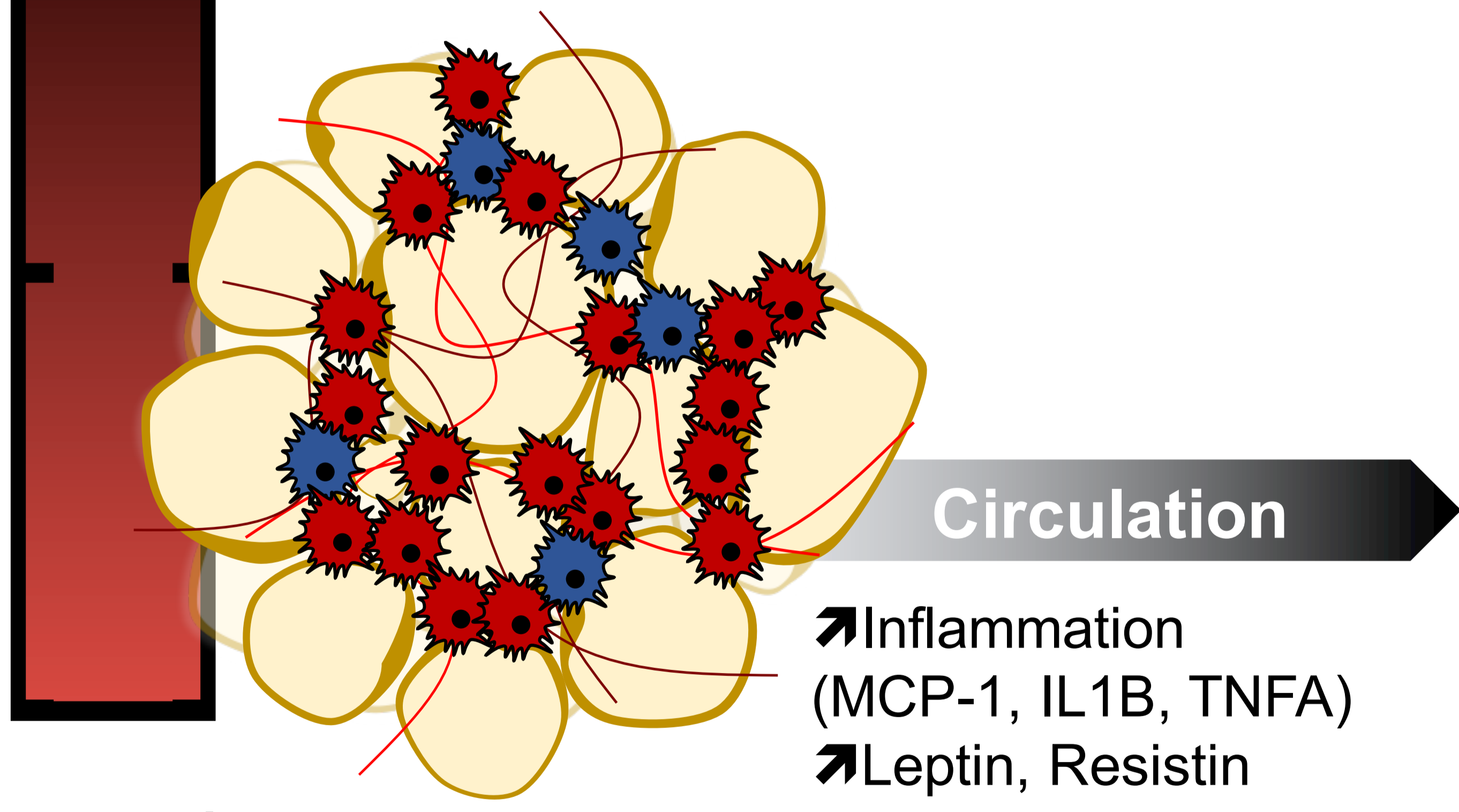
Circulation



↗ Insulin

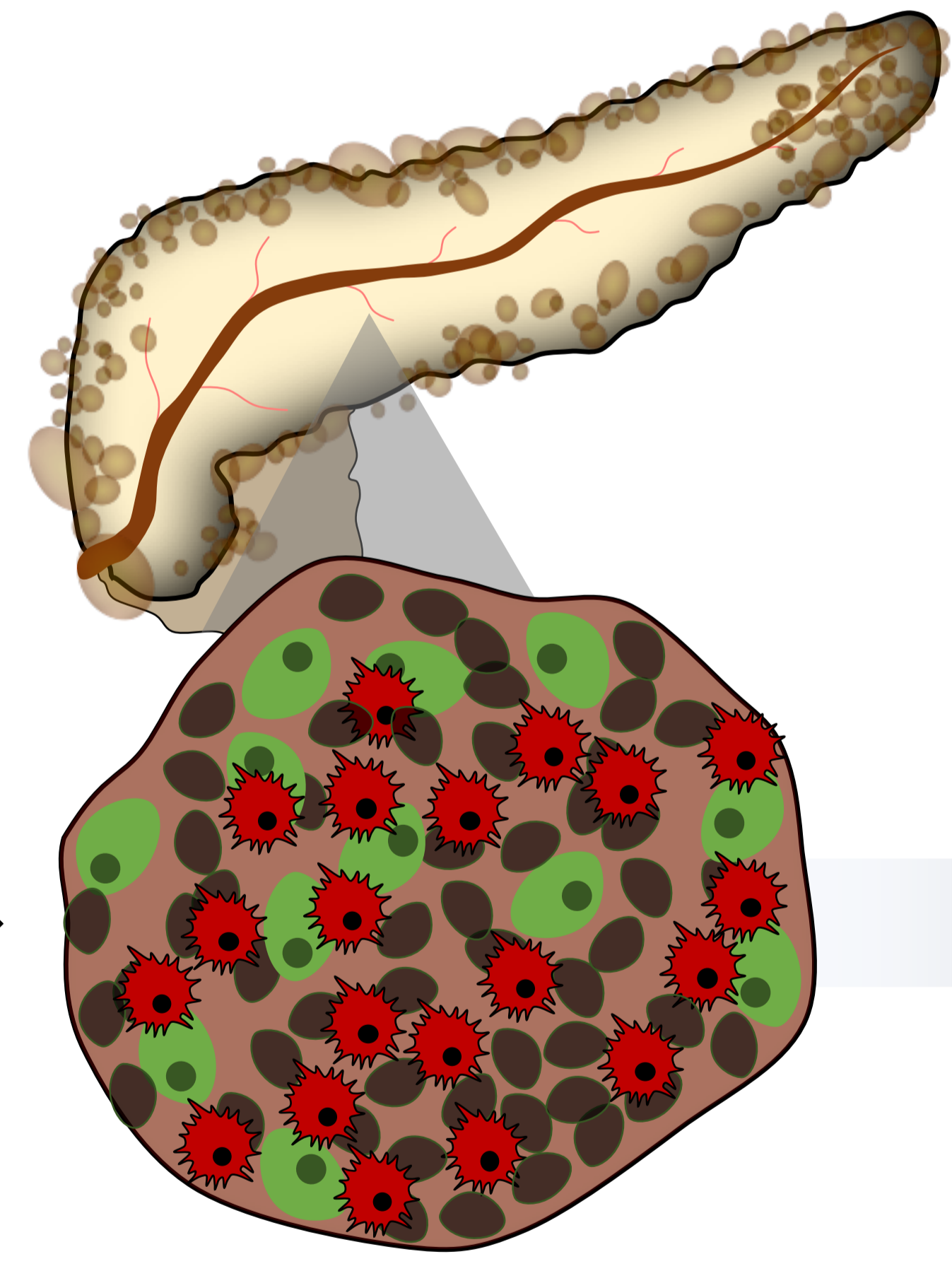
**Controlled-Glycemia
Appropriate Insulin Secretion
Glucose Tolerance**

GPS2^{Lo}



- ↗ Inflammation (MCP-1, IL1B, TNFA)
- ↗ Leptin, Resistin
- ↗ Hypertrophic adipocyte

Circulation



↘ Insulin

**Uncontrolled-Glycemia
Decreased Insulin Secretion
Glucose Intolerance
Pro-Diabetic Status**